Research Journal of Applied Sciences, Engineering and Technology 6(10): 1785-1793, 2013
ISSN: 2040-7459; e-ISSN: 2040-7467

Submitted: November 12, 2012 Accepted: January 21, 2013 Published: July 20, 2013

Mixed Convection Boundary-layer Flow of a Nanofluid Near Stagnation-point on a Vertical Plate with Effects of Buoyancy Assisting and Opposing Flows

[1]Hossein Tamim, [1]Saeed Dinarvand, [1]Reza Hosseini, [1]Sadegh Khalili and [2]Arezoo Khalili
[1]Mechanical Engineering Department, Amirkabir University of Technology, Tehran Polytechnic, 424 Hafez Avenue, Tehran, Iran
[2]Young Researchers Club, Saveh Branch, Islamic Azad University, Saveh, Iran

Abstract: In this study, the steady laminar mixed convection boundary layer flow of a nanofluid near the stagnation-point on a vertical plate with prescribed surface temperature is investigated. Here, both assisting and opposing flows are considered and studied. Using appropriate transformations, the system of partial differential equations is transformed into an ordinary differential system of two equations, which is solved numerically by shooting method, coupled with Runge-Kutta scheme. Three different types of nanoparticles, namely copper Cu, alumina Al_2O_3 and titania TiO_2 with water as the base fluid are considered. Numerical results are obtained for the skin-friction coefficient and Nusselt number as well as for the velocity and temperature profiles for some values of the governing parameters, namely, the nanoparticle volume fraction parameter ϕ and mixed convection parameter λ It is found that the highest rate of heat transfer occurs in the mixed convection with assisting flow while the lowest one occurs in the mixed convection with opposing flow. Moreover, the skin friction coefficient and the heat transfer rate at the surface are highest for copper–water nanofluid compared to the alumina–water and titania–water nanofluids.

Keywords: Boundary layer, mixed convection, nanofluid, numerical solution, stagnation-point flow, similarity transform

INTRODUCTION

Nanofluids are a new class of nanotechnology-based heat transfer fluids engineered by dispersing nanometer-scale solid particles with typical length scales on the order of 1 to 100 *nm* in traditional heat transfer fluids (Das *et al*., 2007). Nanoparticles have different shapes such as: spherical, rod-like or tubular shapes and so on. Choi (1995) was the first who introduced the term of nanofluids to describe this new class of fluid. There are mainly two techniques used to produce nanofluids which are the single-step and the two-step methods (Akoh *et al*., 1978) and Eastman *et al*. (1997). Both of these methods have advantages and disadvantages as discussed by Wang and Mujumdar (2007). The presence of the nanoparticles in the fluids increases appreciably the effective thermal conductivity of the fluid and consequently enhances the heat transfer characteristics. This fact has attracted many researchers such as Abu-Nada (2008), Tiwari and Das (2007), Maïga *et al*. (2005), Oztop and Abu-Nada (2008) and Nield and Kuznetsov (2009) to investigate the heat transfer characteristics in nanofluids.

The concept of a boundary layer is one of the most important ideas in understanding transport processes. The essentials of the boundary-layer theory had been presented in 1904 by Prandtl in a paper that revolutionized fluid mechanics. Free convection is caused by the temperature difference of the fluid at different locations and forced convection is the flow of heat due to the cause of some external applied forces. The combination of free convection and forced convection is called as mixed convection. Mixed convection flows, has many important applications in the fields of science and engineering. The majority of treatments of this problem are limited to cases in which the flow is directed vertically upward (assisting flow), while the situation when the flow is directed downward (opposing flow).

It appears that separation in mixed convection flow was first discussed by Merkin (1969), who examined the effect of opposing buoyancy forces on the boundary layer flow on a semi-infinite vertical flat plate at uniform temperature in a uniform free stream. This problem was studied further by Wilks (1973) and Hunt and Wilks (1980), who also considered the case of uniform flow over a semi-infinite flat plate heated at a constant heat flux rate.

Chen and Mucoglu (1975) have investigated the effects of mixed convection over a vertical slender cylinder due to the thermal diffusion with the prescribed wall temperature and the solution was

Corresponding Author: Saeed Dinarvand, Mechanical Engineering Department, Amirkabir University of Technology (Tehran Polytechnic), 424 Hafez Avenue, Tehran, Iran, Tel.: +98 912 4063341

obtained by using the local non-similarity method. Further, Mahmood and Merkin (1988) have solved this problem using an implicit finite difference scheme. Ishak *et al*. (2007a) analyzed the effects of injection and suction on the steady mixed convection boundary layer flows over a vertical slender cylinder with a free stream velocity and a wall surface temperature proportional to the axial distance along the surface of the cylinder. Grosan and Pop (2011) have studied the axisymmetric mixed convection boundary layer flow past a vertical cylinder.

Among the earlier studies reported in the literature, Ridha (1996), Merkin and Mahmood (1990) and Wilks and Bramley (1981) have studied the mixed convection boundary layer flow over an impermeable vertical flat plate. In such cases, the mixed convection flows are characterized by the buoyancy parameter λ which depends on the flow configuration and the surface heating conditions, where $\lambda > 0$ for assisting flow and $\lambda < 0$ for opposing flow. When the buoyancy effects are negligible, i.e., when $\lambda = 0$, the problem corresponds to forced convection flow past a flat surface.

In modeling boundary layer flows and heat transfer the boundary conditions that are usually applied are either a prescribed surface temperature or a prescribed surface heat flux. Perhaps the simplest case of this is when there is a linear relation between the surface heat transfer and surface temperature. This situation arises in conjugate heat transfer problems (Merkin and Pop, 1996).

Motivated by the above investigations, the present paper studies when the mixed convection boundary layer flow is introduced normal to the vertical plate. The study has been motivated by the need to determine the thermal performance of such a system. A technique for improving heat transfer is using solid particles in the base fluids, which has been used recently in many papers. The term nanofluid refers to fluids in which nano-scale particles are suspended in the base fluid and it has been suggested by Choi (1995). The comprehensive references on nanofluid can be found in the recent book by Das *et al*. (2007) and in the review papers by Buongiorno (2006). Such as above researchers we employed a similarity transformation that reduces the partial differential boundary layer equations to a nonlinear third-order ordinary differential equation before solving it numerically. A large amount of literatures on this problem has been cited in the books by Schlichting and Gersten (2000) and Leal (2007) as well as in the paper by Ishak *et al*. (2007b). We use a numerical technique, combination of shooting method and 4th order Runge-Kutta for solving the governing equations of mixed convection. Finally, we discuss on the effect of solid volume fraction of nanoparticles as well as their types on the fluid flow and heat transfer characteristics and show that nanofluid enhances the thermal conductivity, which is generally low for a regular fluid.

Table 1: Thermophysical properties of the base fluid and the nanoparticles (Oztop and Abu-Nada, 2008)

Physical properties	Fluid phase (water)	Cu	Al_2O_3	TiO_2
C_p(J/kg K)	4179	385	765	686.2
ρ(kg /m^3)	997.1	8933	3970	4250
k(W/mK)	0.613	400	40	8.9538
$\alpha \times 10^{-7}$(m^2/ s)	1.47	1163.1	131.7	30.7

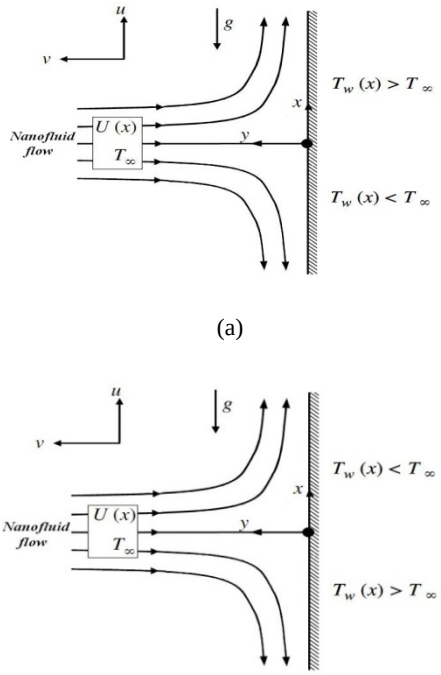

Fig. 1: Physical model of two-dimensional stagnation-point flow on a vertical surface; (a) Assisting flow; (b) Opposing flow

NANOFLUID FLOW ANALYSIS AND MATHEMATICAL FORMULATION

Consider the problem of steady mixed convection boundary layer flow of a nanofluid near the stagnation-point on a vertical flat plate. It is assumed that the nanoparticles are in thermal equilibrium and no slip occurs between them. The thermophysical properties of the fluid and nanoparticles are given in Table 1 (Oztop and Abu-Nada, 2008).

We select a coordinate frame in which x-axis is extending along the surface, while the y-axis is measured normal to the surface of the plate and is positive in the direction from the surface to the fluid (Fig. 1). It is assumed that the x-component velocity of the flow, external to the boundary layer, U(x) and the temperature, $T_w(x)$ of the plate are proportional to the distance from the stagnation-point. $U(x) = \alpha x$ and $T_w(x) = T_\infty + bx$, where α and b are constants with $\alpha > 0$. The assisting flow ($b>0$) occurs if the upper half of the plate is heated while the lower half of the plated is cooled. In

this case, with considering the buoyancy force the flow near the heated plate tends to move upward and the flow near the cooled plate tends to move downward, therefore this behavior acts to assist the main flow field. The opposing flow (b<0) occurs if the upper part of the plate is cooled while the lower part of the plate is heated (Lok *et al*., 2009). Under these assumptions and following the nanofluid model proposed by Tiwari and Das (2007), the governing equations for the continuity, momentum and energy in laminar incompressible boundary layer flow in a nanofluid can be written as:

$$\frac{\partial u}{\partial x}+\frac{\partial v}{\partial y}=0, \tag{1}$$

$$u\frac{\partial u}{\partial x}+v\frac{\partial u}{\partial y}=\frac{\mu_{nf}}{\rho_{nf}}\frac{\partial^2 u}{\partial y^2}-\frac{1}{\rho_{nf}}\frac{dp}{dx}+\frac{\phi\rho_s\beta_s+(1-\phi)\rho_f\beta_f}{\rho_{nf}}g(T-T_\infty), \tag{2}$$

$$u\frac{\partial T}{\partial x}+v\frac{\partial T}{\partial y}=\alpha_{nf}\frac{\partial^2 T}{\partial y^2}, \tag{3}$$

subject to the boundary conditions:

$$\begin{aligned} &u=0, \quad v=0, \quad T=T_w(x) \quad at \quad y=0,\\ &u\to U(x), \quad T\to T_\infty, \quad at \quad y\to\infty. \end{aligned} \tag{4}$$

By employing the generalized Bernoulli's equation, in free-stream, Eq. (2) becomes:

$$U\frac{dU}{dx}=-\frac{1}{\rho_{nf}}\frac{dp}{dx}. \tag{5}$$

Substituting (5), Eq. (2) can be written as:

$$u\frac{\partial u}{\partial x}+v\frac{\partial u}{\partial y}=\frac{\mu_{nf}}{\rho_{nf}}\frac{\partial^2 u}{\partial y^2}+U\frac{dU}{dx}+\frac{\phi\rho_s\beta_s+(1-\phi)\rho_f\beta_f}{\rho_{nf}}g(T-T_\infty). \tag{6}$$

Here, u and v are the velocity components along the x and y axes, respectively, T is the temperature of the nanofluid, β_f and β_s are the thermal expansion coefficients of the base fluid and nanoparticle, respectively, μ_{nf} is the viscosity of the nanofluid, α_{nf} is the thermal diffusivity of the nanofluid and ρ_{nf} is the density of the nanofluid, which are given by:

$$\begin{aligned} &\mu_{nf}=\frac{\mu_f}{(1-\phi)^{2.5}}, \quad \rho_{nf}=(1-\phi)\rho_f+\phi\rho_s, \quad (\rho C_p)_{nf}=(1-\varphi)(\rho C_p)_f+\varphi(\rho C_p)_s\\ &\alpha_{nf}=\frac{k_{nf}}{(\rho C_p)_{nf}}, \quad \frac{k_{nf}}{k_f}=\frac{\left(k_s+2k_f\right)-2\phi\left(k_f-k_s\right)}{\left(k_s+2k_f\right)+\phi\left(k_f-k_s\right)}, \end{aligned} \tag{7}$$

where,

ϕ = The nanoparticle volume fraction

ρ_f = The density of the base fluid

ρ_s = The density of the nanoparticle

μ_f = The viscosity of the base fluid

k_f and k_s = The thermal conductivity of the base fluid and nanoparticle, respectively

k_{nf} = The effective thermal conductivity of the nanofluid approximated by the Maxwell-Garnett model (Oztop and Abu-Nada, 2008)

We look for a similarity solution of Eq. (1), (2) and (3) with the boundary conditions (4) of the following form:

$$\eta=\left(\frac{U}{\upsilon_f x}\right)^{\frac{1}{2}}y, \quad \psi=\left(U\upsilon_f x\right)^{\frac{1}{2}}f(\eta), \quad \theta(\eta)=\frac{T-T_\infty}{T_w-T_\infty}, \tag{8}$$

where, ψ is the stream function and is defined in the usual way as $u = \partial\psi / \partial y$ and $v = -\partial\psi/\partial x$ so as to identically satisfy Eq. (1), and υ_f is the kinematic viscosity of the fluid. By Substituting (8) into Eq. (2) and (3), we obtain the following ordinary differential equations:

$$\frac{1}{(1-\phi)^{2.5}\left(1-\phi+\phi\frac{\rho_s}{\rho_f}\right)}f'''+ff''-f'^2+1+\lambda\theta=0, \tag{9}$$

$$\frac{1}{\Pr}\frac{\frac{k_{nf}}{k_f}}{(1-\phi)+\phi\frac{(\rho C_p)_s}{(\rho C_p)_f}}\theta''+f\theta'-f'\theta=0, \tag{10}$$

subject to the boundary conditions:

$$\begin{aligned} &f(0)=0, \quad f'(0)=0, \quad \theta(0)=1,\\ &f'(\infty)\to 1, \quad \theta(\infty)\to 0. \end{aligned} \tag{11}$$

Here, primes denote differentiation with respect to η,

$\Pr = \upsilon_f / \alpha_f$ is the Prandtl number and λ is the buoyancy or mixed convection parameter, which is defined as:

$$\begin{aligned} &\lambda=\frac{Gr_x}{Re_x^2}=\frac{\phi\rho_s\beta_s+(1-\phi)\rho_f\beta_f}{\rho_{nf}}g\times\frac{b}{a^2},\\ &Gr_x=\frac{\phi\rho_s\beta_s+(1-\phi)\rho_f\beta_f}{\rho_{nf}}g\left(T_w-T_\infty\right)\frac{x^3}{\upsilon_{nf}^2},\\ &Re_x=\frac{Ux}{\upsilon_{nf}}, \end{aligned} \tag{12}$$

where, Gr_x and Re_x are, respectively the local Grashof number and the Reynolds number. We notice that λ is a constant, with $\lambda>0$ and $\lambda<0$ corresponding to assisting and opposing flows, respectively, while $\lambda = 0$ represents the case when the buoyancy force is absent (forced convection).

The physical quantities of interest are the skin friction coefficient a C_f and the local Nusselt number Nu_x, which are defined by:

Table 2: The influence of the different nanoparticle volume fractions on the skin friction coefficient and the Nusselt number for the different nanoparticles, when $\lambda = 1$, 0 and -1

		$\lambda = 1$(*Assisting flow*)		$\lambda = 0$ *(Forced convection*)		$\lambda = -1$ *(Opposing flow*)	
Nanoparticles	ϕ	$[Re_x]^{1/2} C_f$	$[Re_x]^{1/2} Nu_x$	$[Re_x]^{1/2} C_f$	$[Re_x]^{1/2} Nu_x$	$[Re_x]^{1/2} C_f$	$[Re_x]^{1/2} Nu_x$
Cu	0	3.05355	1.65242	2.46518	1.57343	1.82621	1.47787
	0.05	3.91833	1.87279	3.10770	1.77577	2.22075	1.65618
	0.10	4.81536	2.08336	3.76865	1.96921	2.61683	1.82647
	0.15	5.77580	2.29008	4.47381	2.15931	3.03459	1.99394
	0.20	6.82739	2.49642	5.24549	2.34936	3.49056	2.16169
Al_2O_3	0	3.05355	1.65242	2.46518	1.57343	1.82621	1.47787
	0.05	3.51805	1.80652	2.81753	1.71690	2.05421	1.60756
	0.10	4.02763	1.96055	3.20411	1.86033	2.30424	1.73719
	0.15	4.59295	2.11528	3.63365	2.00450	2.58292	1.86760
	0.20	5.22693	2.27145	4.11665	2.15020	2.89819	1.99963
TiO_2	0	3.05355	1.65242	2.46518	1.57343	1.82621	1.47787
	0.05	3.53844	1.78590	2.83469	1.69742	2.06795	1.58950
	0.10	4.06820	1.91667	3.23858	1.81898	2.33229	1.69904
	0.15	4.65406	2.04529	3.68615	1.93870	2.62650	1.80712
	0.20	5.30940	2.17213	4.18844	2.05698	2.95913	1.91423

$$C_f = \frac{\tau_w}{\rho_f U^2/2}, \qquad Nu_x = \frac{xq_w}{k_f(T_w - T_\infty)}, \tag{13}$$

where, the wall shear stress τ_w and the wall heat flux q_w are given by:

$$\tau_w = \mu_{nf}\left(\frac{\partial u}{\partial y}\right)_{y=0}, \qquad q_w = -k_{nf}\left(\frac{\partial T}{\partial y}\right)_{y=0}. \tag{14}$$

Using the similarity variables (8), we obtain:

$$C_f\left[\mathrm{Re}_x\right]^{\frac{1}{2}} = 2\frac{f''(0)}{(1-\varphi)^{2.5}}, \qquad \left[\mathrm{Re}_x\right]^{-\frac{1}{2}} Nu_x = -\frac{k_{nf}}{k_f}\theta'(0). \tag{15}$$

RESULTS AND DISCUSSION

The nonlinear ordinary differential Eq. (9) and (10) subject to the boundary conditions (11) have been solved numerically for some values of the mixed convection parameter λ, volume fraction parameter ϕ as well as the types of nanofluid, by using the combination of shooting method and 4th order Runge-Kutta method. First, we convert the equations into Initial Value Problems (IVPs) by using shooting method. Then the results obtained numerically by 4th order Runge-Kutta method. In this study we have fixed the Prandtl number *Pr* to be 6.2 and also we have considered $\lambda = 1$, 0 and -1. It is worth mentioning that $\lambda = 0$ ($\alpha \to \infty$) corresponds to a forced convection fluid flow and $\lambda \neq 0$corresponds to a mixed convection flow.

We consider three different types of nanoparticles, namely Cu, Al_2O_3 and TiO_2 with water as the base fluid. The thermophysical properties of the base fluid and the nanoparticles are listed in Table 1. Table 2 presents the numerical values of dimensionless skin friction coefficient and local Nusselt number for some values of λ and ∅. It can be noticed that both skin friction coefficient and local Nusselt number increase when all two parameters increase. Also we can say that

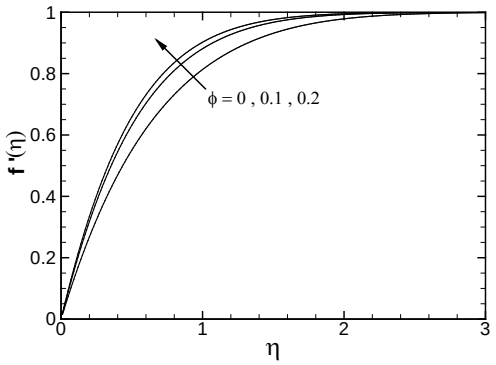

Fig. 2: Velocity profiles $f'(\eta)$ or different values of $\phi$for Cu-water nanofluid when $\lambda = 1$

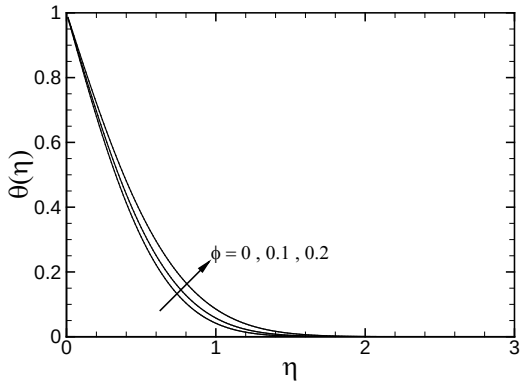

Fig. 3: Temperature profiles θ (η) for different values of ϕ for Cu-water nanofluid when $\lambda = 1$

the shear stress and rate of heat transfer change by using different types of nanofluid. This means that the types of nanofluid will be important in the cooling and heating processes.

Figure 2 show the velocity profiles for various values of the volume fraction parameter ϕ in the case of Cu-water when $\lambda = 1$ (assisting flow). It is noted that the velocity boundary layer decreases with the volume fraction parameter. This is due to the fact that the presence of nano-solid-particles leads to further

thinning of the boundary layer. Figure 3 is presented to show the effect of the nanoparticles volume fraction (Cu) on temperature distribution. From this figure, when the volume of copper nanoparticles increases, the thermal conductivity increases, and then the thermal boundary layer thickness increases.

The effect of the nanoparticles volume fraction on velocity and temperature distributions in the case of Cu-water when $\lambda = 0$ (forced convection) are illustrated in Fig. 4 and 5, respectively. It is observed that the velocity boundary layer decreases while the thermal boundary layer increases when ϕ increases. Comparing with the Fig. 2 and 3, we conclude that the flow strength also increases while the temperature gradient decreases with increasing of buoyancy or mixed convection parameter.

Figure 6 and 7 respectively display the velocity and temperature profiles for different values of $\emptyset$ when $\lambda = -1$ (opposing flow) for Cu-water nanofluid. As shown in these figures, similar to opposing flow and forced convection flow, the velocity boundary layer decreases while the thermal boundary layer increases when ϕ increases. It is evident from these figures that velocity and temperature profiles satisfy the far field boundary conditions asymptotically, thus support the validity of the numerical results obtained. It can be concluded from Fig. 2 to 7 that the highest flow strength or velocity gradient is for $\lambda = 1$ (assisting flow) case while

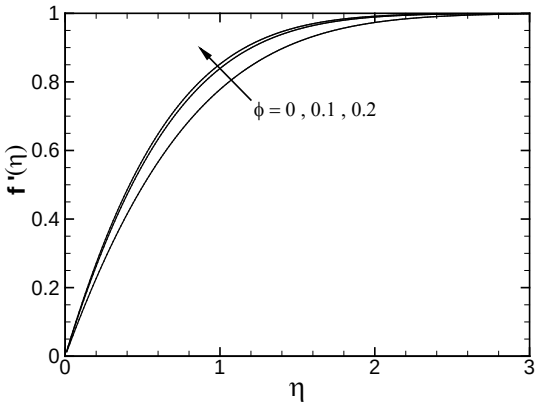

Fig. 4: Velocity profiles $f'(\eta)$ for different values of $\emptyset$ for Cu-water nanofluid when $\lambda = 0$

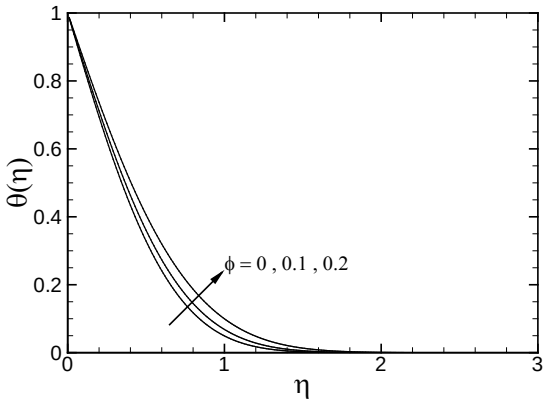

Fig. 5: Temperature profiles $\theta(\eta)$ for different values of ϕ for Cu-water nanofluid when $\lambda = 0$

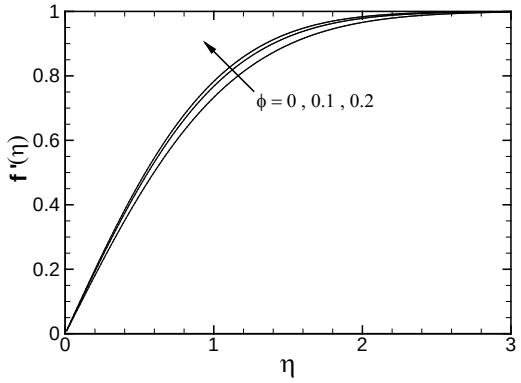

Fig. 6: Velocity profiles $f'(\eta)$ for different values of ϕ for Cu-water nanofluid when $\lambda = -1$

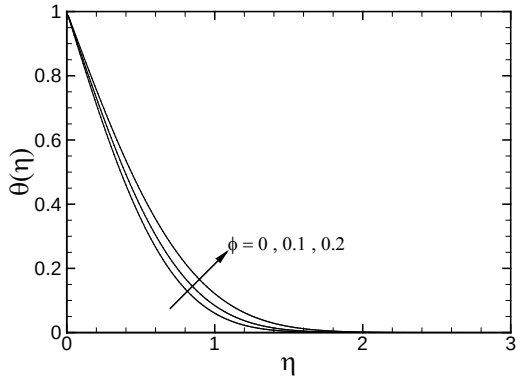

Fig. 7: Temperature profiles $\theta(\eta)$ for different values of $\emptyset$ for Cu-water nanofluid when $\lambda = -1$

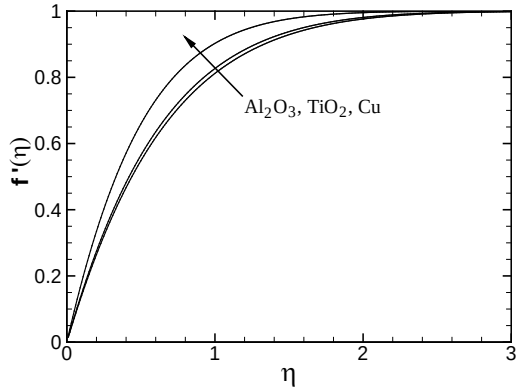

Fig. 8: Velocity profiles $f'(\eta)$ for different nanoparticles when $\phi = 0.2$ and $\lambda = 1$

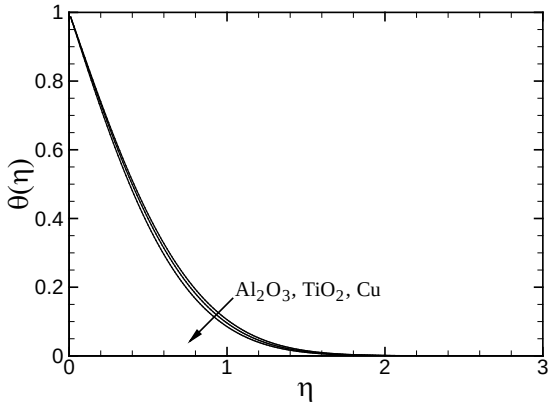

Fig. 9: Temperature profiles θ(η) for different nanoparticles when $\phi = 0.2$ and λ = 1

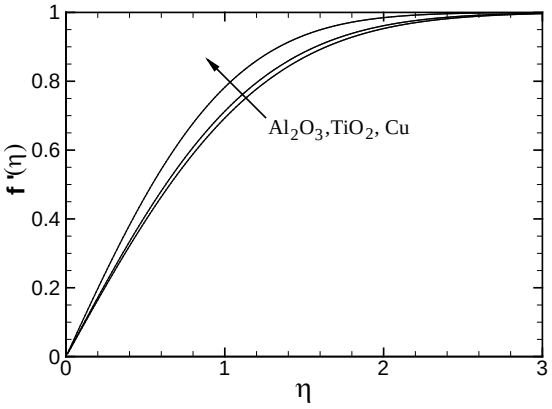

Fig. 12: Velocity profiles $f'(\eta)$ for different nanoparticles when ϕ = 0.2 and λ = -1

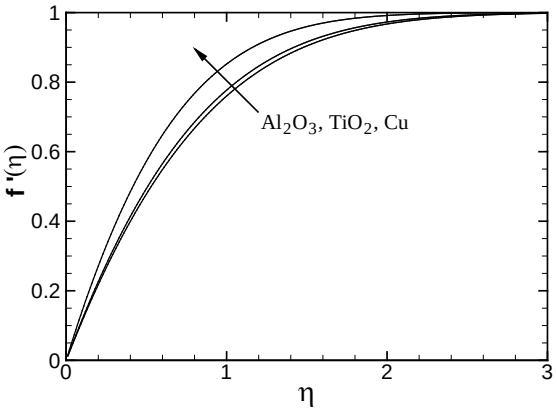

Fig. 10: Velocity profiles $f'(\eta)$ for different nanoparticles when ϕ = 0.2 and λ = 0

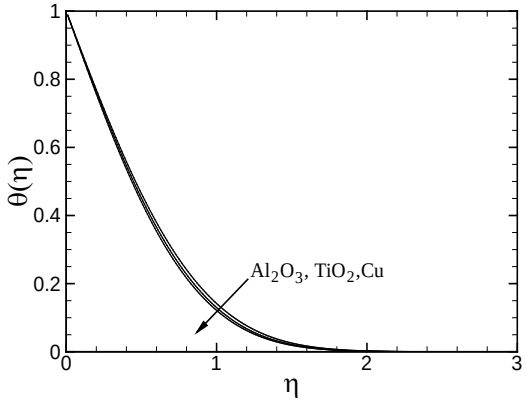

Fig. 13: Temperature profiles $\acute{f}(\eta)$ for different nanoparticles when ϕ = 0.2 and λ = -1

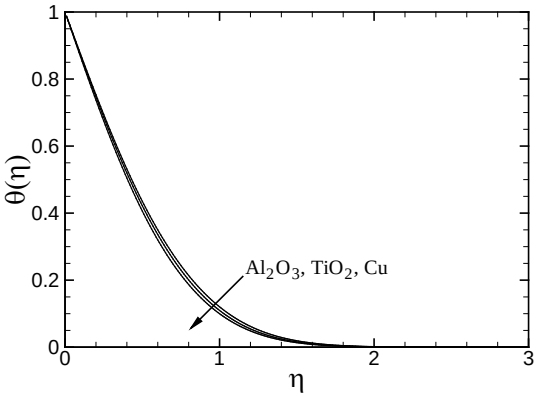

Fig. 11: Temperature profiles θ(η) for different nanoparticles when ϕ = 0.2 and λ = 0

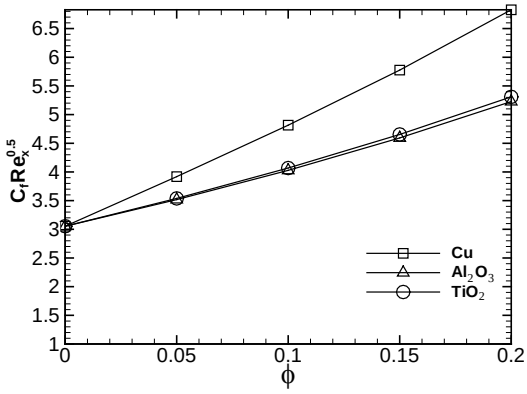

Fig. 14: Variation of the friction coefficient with ϕ for different nanoparticles when λ = 1

the lowest temperature gradient is belong to the same one. This is because, increasing of the buoyancy parameter cause more assisting on the main flow so that the velocity distribution increases and the temperature distribution decreases with increasing λ.

Figure 8 and 9 respectively illustrate the behavior of the velocity and temperature profiles for the different types of nanofluid for λ = 1 (assisting flow) when Pr = 6.2 and ϕ = 0.2 These figures show that by using different types of nanofluid the values of the velocity and temperature change. It is observed that the Cu

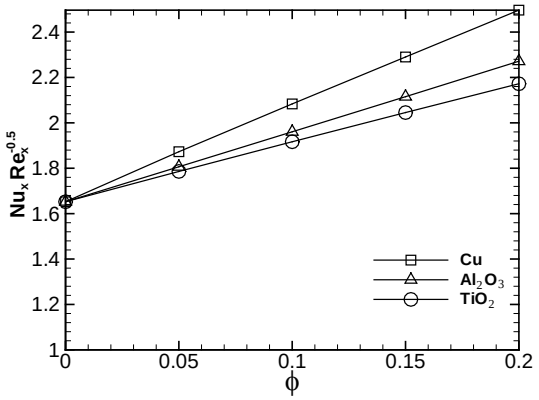

Fig. 15: Variation of the Nusselt number with ϕ for different nanoparticles $\lambda = 1$

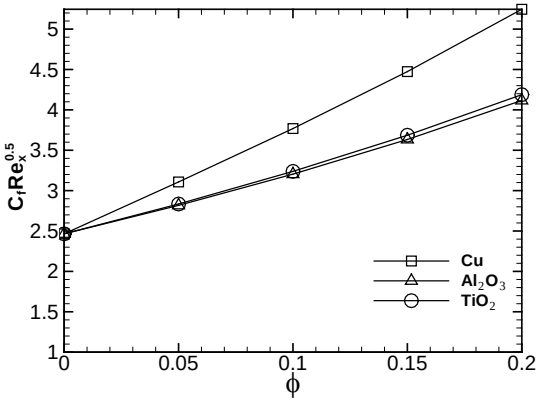

Fig. 16: Variation of the friction coefficient with ϕ for different nanoparticles when $\lambda = 0$

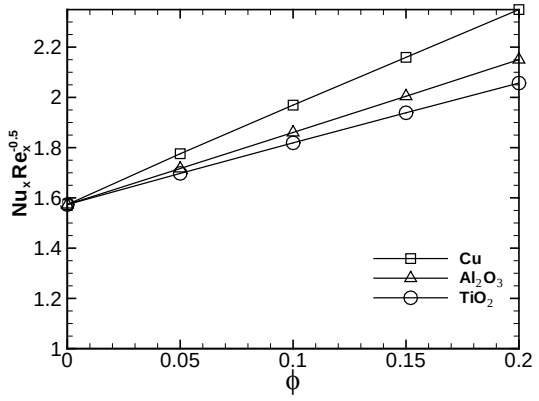

Fig. 17: Variation of the Nusselt number with ϕ for different nanoparticles $\lambda = 0$

nanoparticle (compared to Al_2O_3 and TiO_2) has the smallest velocity and thermal boundary layer. This is because Cu has the highest value of thermal conductivity compared to other nanofluid particles. The reduced value of thermal diffusivity leads to higher temperature gradients and, therefore, higher enhancement in heat transfers. The Cu nanoparticle has higher values of thermal diffusivity (compared to Al_20_3 and $Ti0_2$) and therefore, this reduces the temperature gradients which will affect the performance of Cu nanoparticle.

Figure 10 and 11 respectively show the velocity and temperature profiles for different kind of nanoparticles when $\phi = 0.2$ and $\lambda = 0$ (forced convection). It is shown that Al_2O_3 nanoparticle has the highest velocity and temperature boundary layer while the lowest one is belong to Cu nanoparticle. The thermal conductivity of Al_2O_3 is approximately one tenth of Cu, as given in Table 1. However, a unique property of Al_2O_3 is its low thermal diffusivity. The reduced value of thermal diffusivity leads to higher temperature gradients.

The velocity and temperature profiles for different kind of nanoparticles when $\phi = 0.2$ and $\lambda = - 1$ (opposing flow) are shown in the Fig. 12 and 13, respectively. It is observed that the highest velocity is related to the assisting flow case while the lowest one is for the opposing flow. Unlike the lowest temperature gradient is related to the assisting flow while the highest one is for opposing flow.

Figure 14 and 15 present the variation of the skin friction coefficient and the local Nusselt number for different types of nanofluids when Pr = 6.2 and $\lambda = 1$ (assisting flow), respectively. It is observed that both the skin friction coefficient and the local Nusselt number increase when $\emptyset$ increases and Cu has the highest skin friction coefficient and local Nusselt number compared to TiO_2 and Al_2O_3. It is noted that the lowest heat transfer rate is obtained for the nanoparticles TiO_2 due to the domination of conduction mode of heat transfer. This is because TiO_2 has the lowest value of thermal conductivity compared to Cu and Al_2O_3, as can be seen from Table 1. This behavior of the local Nusselt number (heat transfer rate at the surface) is similar to that reported by Oztop and Abu-Nada (2008). It is also showed that the Al_2O_3 has the lowest skin friction coefficient.

Figure 16 and 17 show the same variation for $\lambda = 0$ (forced convection). As volume fraction of nanoparticles increases, the local Nusselt number and skin friction coefficient become larger especially in the case of assisting flow with respect to the forced convection flow. It is concluded that higher rate of heat transfer occurs in the assisting flow case.

Finally, Fig. 18 and 19 are prepared to present the effect of volume fraction of nanoparticles on the skin friction coefficient and the local Nusselt number for different types of nanofluids in the case of $\lambda = - 1$ (opposing flow), respectively. It is observed from Fig. 14 to 19 that the mixed convection with assisting flow has the highest rate of heat transfer and the mixed convection with opposing flow has the lowest rate of heat transfer.

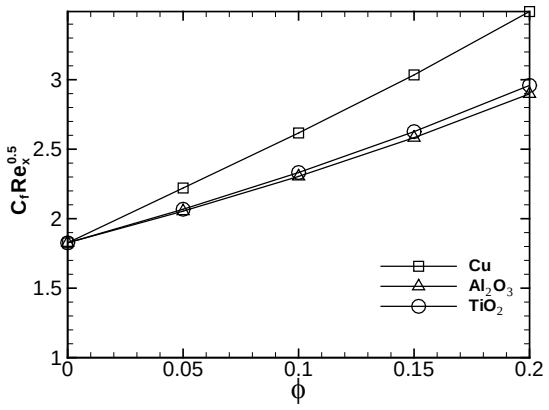

Fig. 18: Variation of the friction coefficient with ϕ for different nanoparticles when $\lambda = -1$

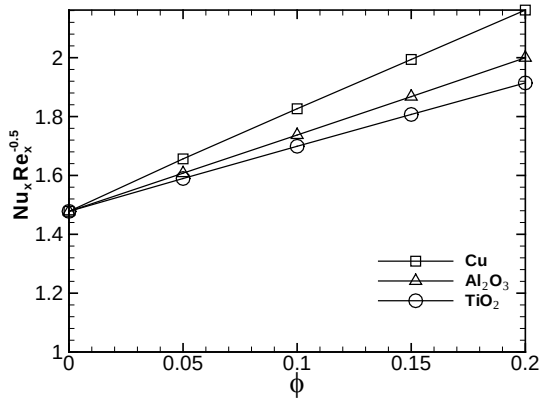

Fig. 19: Variation of the Nusselt number with ϕ for different nanoparticles $\lambda = -1$

FINAL REMARKS

The steady mixed convection boundary layer flow on a vertical plate immersed in a nanofluid with the prescribed external flow and surface temperature were theoretically investigated. The governing partial differential equations were transformed into a system of nonlinear ordinary differential equations using a similarity transformation, before being solved numerically by combination of the shooting method and 4th order Runge–Kutta. The effects of the mixed convection parameter λ and of the solid volume fraction ϕ on the flow and heat transfer characteristics are determined for three kinds of nanofluids: copper (Cu), alumina (Al_2O_3) and titania (TiO_2). Some important points can be drawn from the obtained results such as

- For all values of the mixed convection parameter ($\lambda = 1, 0 - 1$), velocity boundary layer thickness decreases when volume fraction ϕ increases. Besides, the thermal boundary layer thickness increases with the volume fraction parameter.
- The highest value of the velocity and the lowest temperature gradient appear in the case of assisting flow while the lowest velocity and the highest temperature gradient is for opposing flow case.
- The type of nanofluid is a key factor for heat transfer enhancement. The highest values are obtained when using Cu nanoparticles compared to Al_2O_3 and TiO_2 nanoparticles.
- The difference in heat transfer, using different nanofluids, increases with increasing the value of volume fraction of nanoparticles.
- The highest rate of heat transfer occurs in the mixed convection with assisting flow while the lowest one occurs in the mixed convection with opposing flow.
- The effect of solid volume fraction of nanoparticles on the fluid flow and heat transfer characteristics was found to be more pronounced compared to the type of the nanoparticles.

NOMENCLATURE

a, b = Constant
C_f = Skin friction coefficient
g = Acceleration due to gravity
k = Thermal conductivity
Nu_x = Local Nusselt number
Gr_x = Local Grashof number
Re_x = Local Reynolds number
Pr = Prandtl number
q_w = Surface heat flux
T = Fluid temperature
T_w = Surface temperature
T_∞ = Ambient temperature
u, v = Velocity components
x, y = Cartesian coordinates
$U(x)$ = Free stream velocity
$f(\eta)$ = Dimensionless stream function
ϕ = Nanoparticle volume fraction

Greek symbols:

α = Thermal diffusivity
β = Thermal expansion coefficient
η = Similarity variable
$\theta(\eta)$ = Dimensionless temperature
λ = Buoyancy or mixed = convection parameters
μ = Dynamic viscosity
u = Kinematic viscosity
ρ = Fluid density
τ_w = Wall shear stress
ψ = Stream function

Superscripts:

' = Differentiation with respect to η

Subscripts:

w = Condition at the surface of the plate
∞ = Ambient condition

f = fluid
nf = Nanofluid
s = Solid

REFERENCES

Abu-Nada, E., 2008. Application of nanofluids for heat transfer enhancement of separated flows encountered in a backward facing step. Int. J. Heat Fluid Flow, 29: 242-249.

Akoh, H., Y. Tsukasaki and S. Yatsuya, 1978. Magnetic properties of ferromagnetic ultrafine particles prepared by a vacuum evaporation on running oil substrate. J. Crystal. Growth., 45: 495-500.

Buongiorno, J., 2006. Convective transport in nanofluids. ASME J. Heat Transfer, 128: 240-250.

Chen, T.S. and A. Mucoglu, 1975. Buoyancy effects on forced convection along a vertical cylinder. ASME J. Heat Transfer, 97: 198-203.

Choi, S.U.S., 1995. Enhancing thermal conductivity of fluids with nanoparticles. Proceedings of the ASME International Mechanical Engineering Congress. San Francisco, USA, ASME, FED 231/MD., 66: 99-105.

Das, S.K., S.U.S. Choi, W. Yu and T. Pradeep, 2007. Nanofluids: Science and Technology. Wiley, New Jersey.

Eastman, J.A., U.S. Choi, S. Li, L.J. Thompson and S. Lee, 1997. Enhanced thermal conductivity through the development of nanofluids. Proceeding of the Materials Research Society Symposium. Pittsburgh, PA, USA, Boston, MA, USA, 457: 3-11.

Grosan, T. and I. Pop, 2011. Axisymmetric mixed convection boundary layer flow past a vertical cylinder in a nanofluid. Int. J. Heat Mass Transfer, 54: 3139-3145.

Hunt, R. and G. Wilks, 1980. On the behavior of the laminar boundary-layer equations of mixed convection near a point of zero skin friction. J. Fluid Mech., 101: 377-391.

Ishak, A., R. Nazar and I. Pop, 2007a. Falkner-Skan equation for flow past a moving wedge with suction or injection. J. Appl. Math. Comput., 25: 67-83.

Ishak, A., R. Nazar and I. Pop, 2007b. The effects of transpiration on the boundary layer flow and heat transfer over a vertical slender cylinder. Int. J. Non-Linear Mech., 42: 1010-1017.

Leal, L.G., 2007. Advanced Transport Phenomena: Fluid Mechanics and Convective Transport Processes. Cambridge University Press, New York.

Lok, Y.Y., I. Pop, D.B. Ingham and N. Amin, 2009. Mixed convection flow of a micropolar fluid near a non-orthogonal stagnation-point on a stretching vertical sheet. Int. J. Numer. Meth. Heat Fluid Flow., 19: 459-483.

Mahmood, T. and J.H. Merkin, 1988. Mixed convection on a vertical circular cylinder. Appl. Math. Phys. (ZAMP), 39: 186-203.

Maïga, S.E.B., S.J. Palm, C.T. Nguyen, G. Roy and N. Galanis, 2005. Heat transfer enhancement by using nanofluids in forced convection flows. Int. J. Heat Fluid Flow., 26: 530-546.

Merkin, J.H., 1969. The effect of buoyancy forces on the boundary-layer flow over a semi-infinite vertical flat plate in a uniform free stream. J. Fluid Mech., 35: 439-450.

Merkin, J.H. and I. Pop, 1996. Conjugate free convection on a vertical surface. Int. J. Heat Mass Transfer., 39: 1527-1534.

Merkin, J.H. and T. Mahmood, 1990. On the free convection boundary layer on a vertical plate with prescribed surface heat flux. J. Eng. Math., 24: 95-107.

Nield, D.A. and A.V. Kuznetsov, 2009. The chenge-minkowycz problem for natural convective boundary-layer flow in a porous medium saturated by a nanofluid. Int. J. Heat Mass Transfer., 52: 5792-5795.

Oztop, H.F. and E. Abu-Nada, 2008. Numerical study of natural convection in partially heated rectangular enclosures filled with nanofluids. Int. J. Heat Fluid Flow., 29: 1326-1336.

Ridha, A., 1996. Aiding flows non-unique similarity solutions of mixed-convection boundary-layer equations. J. Appl. Math. Phys. (ZAMP), 47: 341-352.

Schlichting, H. and K. Gersten, 2000. Boundary-layer Theory. Rev. 8th Edn., Springer, Berlin, London.

Tiwari, R.J. and M.K. Das, 2007. Heat transfer augmentation in a two-sided lid-driven differentially heated square cavity utilizing nanofluids. Int. J. Heat Mass Transfer., 50: 2002-2018.

Wang, X.Q. and A.S. Mujumdar, 2007. Heat transfer characteristics of nanofluids: A review. Int. J. Thermal Sci., 46: 1-19.

Wilks, G., 1973. Combined forced and free convection flow on vertical surfaces. Int. J. Heat Mass Transfer., 16: 1958-1963.

Wilks, G. and J.S. Bramley, 1981. Dual solutions in mixed convection. P. Roy. Soc. Edinb. A, 87A: 349-358.